Robotica (1998) volume 16, pp. 669–677. Printed in the United Kingdom © 1998 Cambridge University Press

Self-motion utilization for reducing vibration of a structurally flexible redundant robot manipulator system

Seon-Jae Kim and Youn-Sik Park

Center for Noise and Vibration Control, Department of Mechnical Engineering, Korea Advanced Institute of Science and Technology, Science Town, Taejon 305–701, Korea

(Received in Final Form: February 17, 1998)

SUMMARY

This paper focuses on overcoming the problem of tracking control in structurally flexible redundant manipulators by utilizing their self-motion capabilities. In the proposed algorithm, the self-motion is evaluated in order to nullify the dominant modal force of flexural motion that is induced by a rigid body motion.

The flexure motions of manipulators, which are induced by joint motion, cause undesired inaccuracy in end-effector tracking. In-plath planning states, joint trajectories are so designed as not to excite but to damp out the flexure motions. The self-motion, inherent in redundant manipulators, can alter joint motion, influencing the flexure motion (by exciting and damping the flexure modes), while not affecting end-effector motion at all. Therefore, the self-motion can be utilized to regulate flexibility and effectively reduce the end-effector tracking error.

The effectiveness and applicability of the proposed algorithm have been demonstrated through numerical simulation with three-link planar robotic manipulators possessing flexible links.

KEYWORDS: Redundant manipulators; Redundancy resolution; Flexible manipulators; Vibration reduction; Self-motion utilizatoin; Modal force nullification

1. INTRODUCTION

Due to its self-motion capability, redundant manipulators have the potential to avoid singularity, obstacles, structural limitation, and so on. They can also carry out reasonable action while performing the main task, for example, tracking a given end-effector trajectory. Because of their higher dexterity and versatility, redundant manipulators have been an appealing research topic in robotics. Many redundancy resolution algorithms have been proposed as tools for a wide variety of robotic problems.

A survey paper of these algorithms is presented by Nenchev.[1] The works mentioned in Nenchev's survey have been associated mainly with rigid link manipulators. However, as the demand for lighter and more versatile robots has increased, numerous research studies on analysis and control of flexible manipulators (as summarized by Book[2]) have been advanced. Of course, these approaches may be used for flexible manipulators with redundancy. However, with the exeption of Nguyen and Walker,[3] little attention has been paid to the issue of how to control flexible effects by using the extra maneuverability inherent in redundant manipulators. The key question is how to choose the self-motion of structurally flexible redundant manipulators to prevent undesired flexibility effects.

Recognizing that joint motion (the main source of system vibration) will excite or reduce flexibility effects through dynamic coupling, the joint trajectories are designed not to excite the natural modes but to reduce the flexure motion. In the redundant manipulator, joint motion (including the self-motion), is crucially important to vibration reduction. The self-motion enables the flexure motion to be altered while it does not affect end-effector motion. Since the redundant manipulator possesses infinite configurations for a given end-effector motion, this self-motion capability enables one to select proper configuration histories from the infinite candidates from the standpoint of vibration reduction. The self-motion alters the dynamic response of flexible arms, while maintaining an end-effector tracking a given trajectory. It helps to effectively reduce the end-effector tracking error.

As far as we know, not many studies have been done on structurally flexible redundant manipulators. Barbieri and Wang,[4] Carusone and D'Eleuterio,[5] propoosed an optimal PI controller to reduce the end-effector tracking error for redundant flexible manipulators. However, these studies did not explicitly address the relationship between self-motion and flexural motion; they merely considered self-motion control within a framework of optimal controller design. Yoshikawa et al.[6] proposed a quasi-static control law for a macro-micro system. Redundancy is utilized to maximise the compensability measure, but they used a simple kinematic analysis to account for its flexibility.

Nguyen and Walker[3] studied how kinematic redundancy affects managing the flexibility of manipulators. They demonstrated how choosing the self-motion inherent in redundant arms is critically important when flexibility is present. A new control algorithm was proposed to regulate flexibility while maintaining the precise tracking of the end-effector trajectory. In their control algorithm the self-motion was used to compensate and damp out flexure motion. Through simulation results, they showed that self-motion can be used to compensate for flexibility in some cases (when the degree of redundancy (DOR) is the same as the number of modes desired to control). They concluded that this control approach can be used to aid in planning joint space trajectories that use the redundancy to reduce the effects of flexibility.

https://doi.org/10.1017/S0263574798000770 Published online by Cambridge University Press

In this paper we aim to develop an efficient control algorithm to prevent motion-induced vibration by utilizing the self-motion inherent in flexible redundant manipulators. We investigate the self-motion effects on flexure motion in modal space as an extension of the work done by Nguyen and Walker. Generally, the available DOR is restricted to one or two but the number of the degree of freedom (DOF) of flexure motion is much greater than the available DOR. Thus, modal space is introduced to reduce the flexure DOF without loss of accuracy. To prevent flexibility effects but not affecting end-effector motion, the self-motion is evaluated to nullify the dominant nodal force induced by rigid body motion.

The authors of this paper, Kim and Park,[7] propose an efficient algorithm which resolves the redundancy for reducing flexibility effects. A concept of modal space is introduced to reduce the degree of freedom of flexure motion. The research shows effective vibration reduction even when the available degree of redundancy is restricted to one or two.

The paper is organized as follows: in section 2, the kinematic and dynamic model of flexible redundant manipulators is obtained. In section 3, the study of Nguyen and Walker[3] is briefly mentioned. After investigating the self-motion effects on flexural motion in modal space, a new efficient algorithm for reducing vibration in utilizing self-motion capbility is proposed. Considering tht the available degree of redundancy is restricted to one or two, a concept of modal space is applied to reduce the system degree of freedom. In section 4, through the numerical simulation with structurally flexible three-link planar flexible manipulators in comparison with the Nguyen and Walker's method,[3] the effectiveness and applicability of the suggested method have been evaluated. Concluding remarks are given in section 5.

2. DYNAMIC AND KINEMTIC MODELLING

We shall model a structurally flexible redundant manipulator (Figure 1), consisting of n_r joints and operating in an m dimensional work space. Let $\boldsymbol{\theta} \in R^{n_r}$ be the set of rigid DOF associated with the joint motion and $\boldsymbol{q} \in R^{n_q}$ be the set of flexural DOF used to represent the elastic deformation in a flexible link.

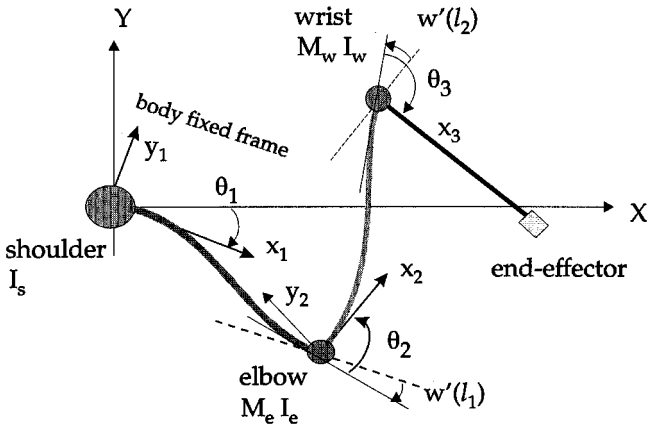


Fig. 1. The planar structurally flexible redundant manipulator and its initial configuration.

Table I. The model parameters for planar flexible redundant manipulator

link	first	second	third
L_i (m)	1.0	1.0	1.0
$m_i(kg/m)$	0.5	0.5	0.25
EI_i	80.0	60.0	∞
mass(kg)	∞	$M_e = 0.1$	$M_w = 0.025$
moment of inertia (kgm^2)	$I_s = 0.85$	$I_e = 0.025$	$I_w = 0.01$

Using the assumed mode method, the elastic deformation of the flexible links can be represented with the summation of spatial mode function $\phi_{i,k}$ and time varying amplitude $q_{i,k}$

$$w_i(x_i, t) = \sum_{k=1}^{n_i} \phi_{i,k}(x_i) q_{i,k}(t) \tag{1}$$

with respect to a reference frame $\{x_i, y_i\}$ attached to the flexible link at the joint. The spatial mode function can be selected freely using, for example, a cantilever mode[8] (clamped-free) function as is done in this work.

The dynamic equation of motion[9] for a general flexible manipulator having $n(n = n_r + n_q)$ DOF can be derived from Lagrange equation and can be represented as

$$\boldsymbol{M}(\boldsymbol{\theta}, \boldsymbol{q}) \begin{Bmatrix} \ddot{\boldsymbol{\theta}} \\ \ddot{\boldsymbol{q}} \end{Bmatrix} + \boldsymbol{D}(\boldsymbol{\theta}, \boldsymbol{q}) \begin{Bmatrix} \dot{\boldsymbol{\theta}} \\ \dot{\boldsymbol{q}} \end{Bmatrix} + \boldsymbol{K}(\boldsymbol{\theta}, \boldsymbol{q}) \begin{Bmatrix} \boldsymbol{\theta} \\ \boldsymbol{q} \end{Bmatrix} + \boldsymbol{N}(\boldsymbol{\theta}, \dot{\boldsymbol{\theta}}, \boldsymbol{q}, \dot{\boldsymbol{q}})$$

$$= \begin{Bmatrix} \boldsymbol{I}_{n_r} \\ \boldsymbol{B}_q \end{Bmatrix} \boldsymbol{\tau} \tag{2}$$

where $\boldsymbol{M}(\boldsymbol{\theta}, \boldsymbol{q}) \in R^{n \times n}$ is the inertia matrix, $\boldsymbol{D}(\boldsymbol{\theta}, \boldsymbol{q}) \in R^{n \times n}$ is the damping matrix, $\boldsymbol{K}(\boldsymbol{\theta}, \boldsymbol{q}) \in R^{n \times n}$ is the stiffness matrix, and $N \in R^n$ is the sum of nonlinear forces such as Coriolis, gravitational, and centrifugal force terms. $\boldsymbol{\tau} \in R^{n_r}$ is the control torque applied to the joints. $\boldsymbol{B}_q \in R^{n_q \times n_r}$ is the input matrix composed of bending slopes at the base of each flexible link. Thus, it depends on the spatial mode function representing the deformation of flexible link. When a cantilever mode function is used as in this work, the input matrix becomes zero, which means the joint torque cannot directly excite the flexure motion. Representing the manipulator motion in two parts, rigid body and flexural motion of flexible links, the equation of motion can be divided into two equations:

$$\boldsymbol{M}_{rr}\ddot{\boldsymbol{\theta}} + \boldsymbol{M}_{rq}\ddot{\boldsymbol{q}} + N_r = \boldsymbol{\tau} \tag{3}$$

$$\boldsymbol{M}_{qr}\ddot{\boldsymbol{\theta}} + \boldsymbol{M}_{qq}\boldsymbol{z}\ddot{\boldsymbol{q}} + \boldsymbol{D}_{qq}\boldsymbol{q} + \boldsymbol{K}_{qq}\boldsymbol{q} + N_q = \boldsymbol{0}_{n_q} \tag{4}$$

where subscript r and q means rigid body and flexural motion, respectively. $\boldsymbol{M}_{rr} \in R^{n_r \times n_r}$, $\boldsymbol{M}_{rq} \in R^{n_r \times n_q}$, and $\boldsymbol{M}_{qq} \in R^{n_q \times n_r}$ are sub-block matrices of the inertia matrix. It is assumed that the rigid degrees of freedom have no damping and stiffness.

The position of the end-effector in an m dimensional work space is expressed by the kinematic equation. It is a

https://doi.org/10.1017/S0263574798000770 Published online by Cambridge University Press

function of both rigid and flexural degrees of freedom:

$$\boldsymbol{x}=\boldsymbol{f}(\boldsymbol{\theta},\boldsymbol{q}) \tag{5}$$

where $\boldsymbol{x}\in R^m$.

The end-effector velocity and acceleration can be obtained by differentiating equation (5) with respect to time, resulting in

$$\dot{\boldsymbol{x}}=\frac{\partial \boldsymbol{f}}{\partial \boldsymbol{\theta}}\dot{\boldsymbol{\theta}}+\frac{\partial \boldsymbol{f}}{\partial \boldsymbol{q}}\dot{\boldsymbol{q}}=\boldsymbol{J}_r\dot{\boldsymbol{\theta}}+\boldsymbol{J}_q\dot{\boldsymbol{q}} \tag{6}$$

$$\ddot{\boldsymbol{x}}=\boldsymbol{J}_r\ddot{\boldsymbol{\theta}}+\boldsymbol{J}_q\ddot{\boldsymbol{q}}+\dot{\boldsymbol{J}}_r\dot{\boldsymbol{\theta}}+\dot{\boldsymbol{J}}_q\dot{\boldsymbol{q}} \tag{7}$$

where $\boldsymbol{J}_r\in R^{m\times n_r}$ and $\boldsymbol{J}_q\in R^{m\times n_q}$ are the Jacobian matrices with respect to rigid body motion and flexural motion, respectively.

The end-effector motion is influenced by both rigid and flexural motion. However, the rigid and the flexural motions are coupled dynamically, as represented in equations (3)–(4), and the flexural DOF cannot be controlled directly by the joint torque. Thus, we may simplify the model in assuming that the resolution of redundancy is influenced by rigid body motion only. Then, the end-effector acceleration becomes

$$\ddot{\boldsymbol{x}}=\boldsymbol{J}_r\ddot{\boldsymbol{\theta}}+\dot{\boldsymbol{J}}_r\dot{\boldsymbol{\theta}}. \tag{8}$$

Since $\boldsymbol{J}_r\in R^{m\times n_r}$ and $n_r>m$, the DOR ρ is defined as

$$\rho=n_r-m, \tag{9}$$

the general solution for $\ddot{\boldsymbol{\theta}}$ is represented by the pseudo-inverse of $\boldsymbol{J}_r$, $\boldsymbol{J}_r^+$, and the basis matrix of the null space of $\boldsymbol{J}_r$, $\boldsymbol{Z}$, which can be calculated using the method proposed by Chang.[10]

$$\ddot{\boldsymbol{\theta}}=\boldsymbol{J}_r^+(\ddot{\boldsymbol{x}}-\dot{\boldsymbol{J}}_r\dot{\boldsymbol{\theta}})+\boldsymbol{Z}\boldsymbol{\varepsilon} \tag{10}$$

where $\boldsymbol{J}_r^+=\boldsymbol{J}_r^T(\boldsymbol{J}_r\boldsymbol{J}_r^T)^{-1}\in R^{n_r\times m}$ and $\boldsymbol{Z}\in R^{n_r\times \rho}$.

Since $\boldsymbol{\varepsilon}\in R^\rho$ is an arbitrary real vector and it determines null space motion, there is an infinite number of solutions for $\ddot{\boldsymbol{\theta}}$, depending on the self-motion vector $\boldsymbol{\varepsilon}$. The self-motion alters the joint motions while not affecting the end-effector motion.

Recognizing that the flexural motion is basically induced by the applied rigid body motion, the altered joint motion can excite or reduce the motion-induced vibration. In the case of a redundant manipulators, such altered joint motion, depending on the self-motion vector $\boldsymbol{\varepsilon}$, is performed in the null space of the Jacobian matrix. As a result, the dynamics of flexure motion can be influenced by maintaining end-effector tracking along a given continuous path.

3. REDUNDANCY RESOLUTION FOR VIBRATION REDUCTION

3.1. Flexure motion compensation and damping

The joint acceleration required to track the desired end-effector motion $\boldsymbol{x}_d$, including the tracking error feedeback, is obtained from equation (10). Then the corresponding joint torque can be calculated by substituting equation (10) into the rigid body motion equation (3):

$$\boldsymbol{\tau}_{com}=\boldsymbol{M}_{rr}\boldsymbol{J}_r^+(\ddot{\boldsymbol{x}}_d+\boldsymbol{k}_v\dot{\boldsymbol{e}}+\boldsymbol{k}_p\boldsymbol{e}-\dot{\boldsymbol{J}}_r\dot{\boldsymbol{\theta}})+\boldsymbol{M}_{rr}\boldsymbol{Z}\boldsymbol{\varepsilon}+\boldsymbol{M}_{rq}\ddot{\boldsymbol{q}}+\boldsymbol{N}_r \tag{11}$$

where $\boldsymbol{e}=(\boldsymbol{x}_d-\boldsymbol{x})$ is the tracking error of the end-effector, $\boldsymbol{k}_v\in R^{m\times m}$ and $\boldsymbol{k}_p\in R^{m\times m}$ are constant feedback gain matrices.

The joint acceleration due to the computed torque can be calculated by substituting equation (11) into the equation of rigid body motion

$$\ddot{\boldsymbol{\theta}}=\boldsymbol{M}_{rr}^{-1}(\boldsymbol{\tau}_{com}-\boldsymbol{N}_r-\boldsymbol{M}_{rq}\ddot{\boldsymbol{q}}). \tag{12}$$

By substituting equation (12) into the flexural motion equation (equation(4)) and then combining it with equation (11), the governing equation becomes

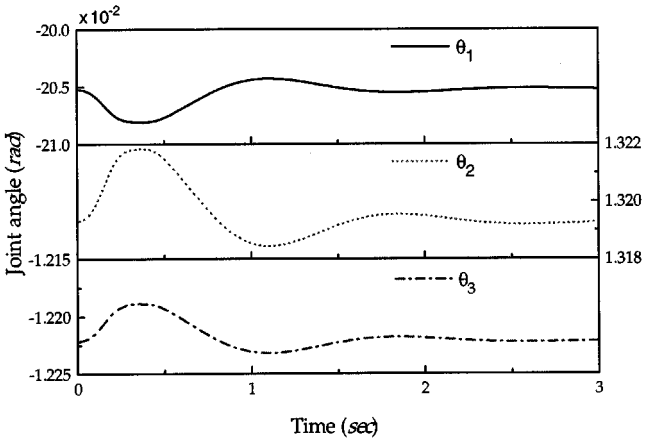
$$\begin{aligned}\boldsymbol{M}_{qq}\ddot{\boldsymbol{q}}+\boldsymbol{D}_{qq}\dot{\boldsymbol{q}}+\boldsymbol{K}_{qq}\boldsymbol{q}&\\ =-\boldsymbol{M}_{qr}\ddot{\boldsymbol{\theta}}-\boldsymbol{N}_q&\\ =-\boldsymbol{M}_{qr}\boldsymbol{J}_r^+(\ddot{\boldsymbol{x}}_d+\boldsymbol{k}_v\dot{\boldsymbol{e}}+\boldsymbol{k}_p\boldsymbol{e}-\dot{\boldsymbol{J}}_r\dot{\boldsymbol{\theta}})-\boldsymbol{M}_{qr}\boldsymbol{Z}\boldsymbol{\varepsilon}-\boldsymbol{N}_q&\end{aligned} \tag{13}$$

The right hand side (r.h.s.) of equation (13) can be interpreted as the exciting force due to the rigid body motion. We can make this term zero by properly selecting the self-motion vector ($\boldsymbol{\varepsilon}$). The flexure motion then becomes a free vibration problem with initial conditions, such as,

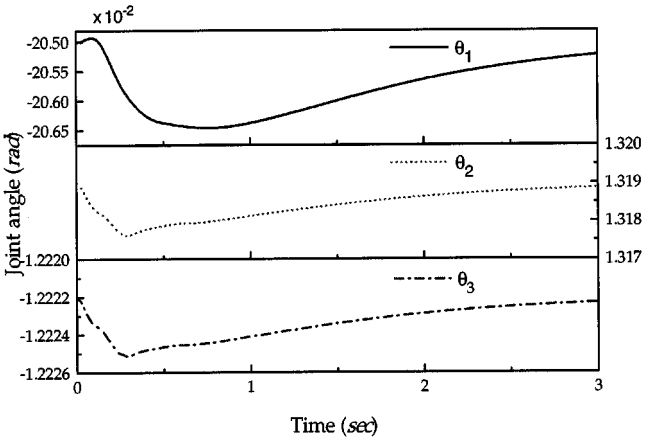
$$\boldsymbol{M}_{qq}\ddot{\boldsymbol{q}}+\boldsymbol{D}_{qq}^d\dot{\boldsymbol{q}}+\boldsymbol{K}_{qq}\boldsymbol{q}=\boldsymbol{0}, \qquad \text{with } \boldsymbol{q}(0) \text{ and } \dot{\boldsymbol{q}}(0) \tag{14}$$

where $\boldsymbol{D}_{qq}^d$ is the desired damping matrix.

The self-motion vector, nullifying the inertia force of rigid body motion, can be obtained by solving the following



(a) The self-motion utilization



(b) The full state feedback

Fig. 2. Comparison of joint trajectory (solid line: θ_1, dot line: θ_2, dash-dot line: θ_3).

https://doi.org/10.1017/S0263574798000770 Published online by Cambridge University Press

set of equations:

$$\underbrace{\boldsymbol{M}_{qr}\boldsymbol{Z}\boldsymbol{\varepsilon}}_{\boldsymbol{H}\cdot\boldsymbol{\varepsilon}} = \underbrace{-\boldsymbol{N}_q - \boldsymbol{M}_{qr}\boldsymbol{J}_r^{+}(\ddot{\boldsymbol{x}}_d + \boldsymbol{k}_v\dot{\boldsymbol{e}} + \boldsymbol{k}_p\boldsymbol{e} - \dot{\boldsymbol{J}}_r\dot{\boldsymbol{q}}) - (\boldsymbol{D}_{qq} - \boldsymbol{D}_{qq}^{D})\dot{\boldsymbol{q}}}_{\boldsymbol{b}} \tag{15}$$

Equation (15) represents n_q equations with ρ unkowns ε. The rank of matrix $\boldsymbol{H}$ is min(n_q,ρ). Realizing that, generally and practically, flexural DOF (n_q) is far greater than the degree of redundancy (ρ), the rank of matrix $\boldsymbol{H}$ can be set ρ and the self-motion vector can be calculated in a least squares sense.[3]

$$\boldsymbol{\varepsilon} = \boldsymbol{H}^{+}\boldsymbol{b} = (\boldsymbol{H}^{T}\boldsymbol{H})^{-1}\boldsymbol{H}^{T}\boldsymbol{b} \tag{16}$$

Since the solution is a least squares one, it cannot perfectly cancel the r.h.s. Some error always remains in all the flexural DOF.

3.2. Redundancy resolution in instantaneous modal space

As seen from equation (15), the same number of DOR along with flexural DOF are required in order to perfectly nullify the entire exciting force. However, this is not practical. Since the magnitude of several low frequency components of flexural motion is considerably larger than those of all the remaining high frequency components, the high frequency terms can be neglected. Thus, only several low frequency modes are selected to nullify their modal forces.

Adjoining the identity $\dot{\boldsymbol{q}} = \dot{\boldsymbol{q}}$, the flexure motion equation (13) can be written in states space form[11] at a specific time t^*,

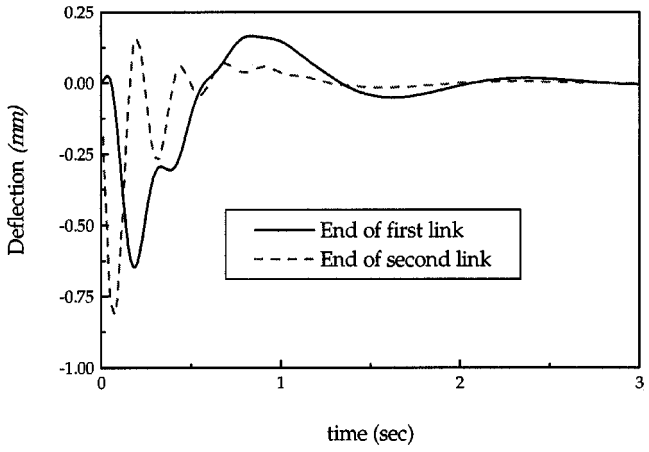
$$\dot{\boldsymbol{Y}}^* = \boldsymbol{A}^*\boldsymbol{Y}^* + \boldsymbol{B}^*\boldsymbol{f}_c^* \tag{17}$$

where $\boldsymbol{Y}^* = [\boldsymbol{q}^T(t^*)\dot{\boldsymbol{q}}^T(t^*)]^T$ is the state vector and

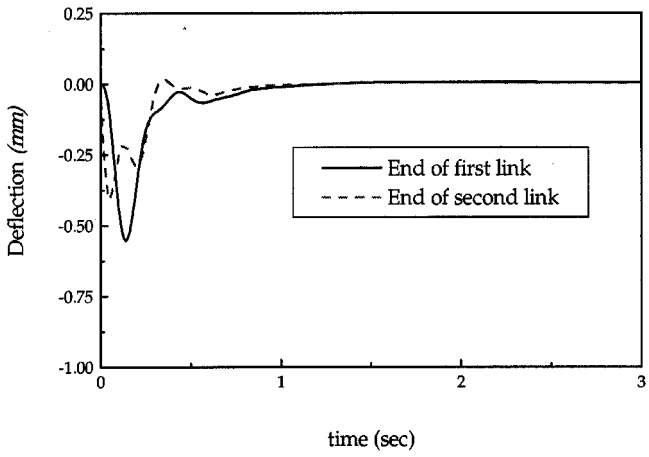
$$\boldsymbol{A}^* = \begin{bmatrix} \boldsymbol{0} & \boldsymbol{I} \\ -\boldsymbol{M}_{qq}^{*-1}\boldsymbol{K}_{qq}^{*} & -\boldsymbol{M}_{qq}^{*-1}\boldsymbol{D}_{qq}^{*} \end{bmatrix},\ \boldsymbol{B}^* = \begin{bmatrix} \boldsymbol{0} \\ -\boldsymbol{M}_{qq}^{*-1} \end{bmatrix} \tag{18a,b}$$

Note from the notation $\boldsymbol{f}_c^{+}$ represents the r.h.s. of the equation (13). Our objective is to transform equation (17) into a set of quasi-static modal equations. The Quasi-static analysis[12] is performed to get the instantaneous modal properties in time-varying systems. It is based on the assumption that the eigenvectors are kept constant in a given instant.

Let us use the expansion theorem and express the solution of equation (17) as a linear combination of the right eigenvectors multiplied by time dependent modal coor-

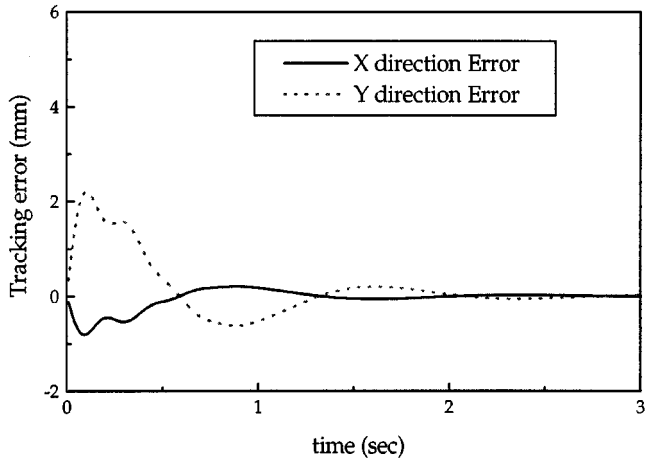


(a) The self-motion utilization

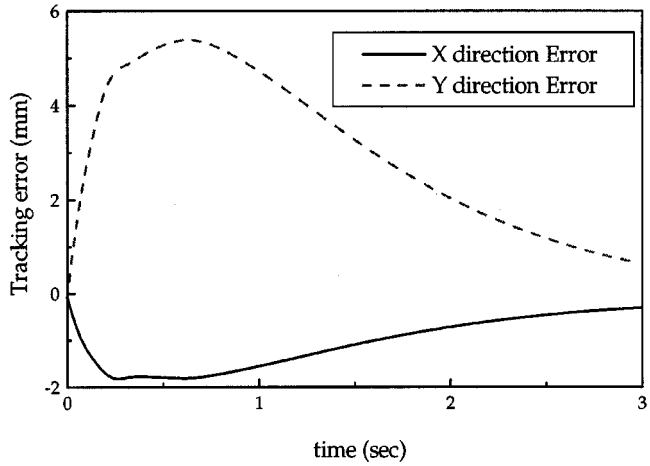


(b) The full state feedback

Fig. 3. Comparison of the deflection at the end of the first link and second link (solid line: the first link, dashed line: the second link)



(a) The self-motion utilization



(b) The full state feedback

Fig. 4. Comparison of the end-effector position error (solid line: X direction error, dashed line: Y direction error)

https://doi.org/10.1017/S0263574798000770 Published online by Cambridge University Press

dinates as follows:

$$\mathbf{Y}^* = \sum_{i=1}^{2n_q} \eta_i(t^*)\mathbf{u}_i = \mathbf{U}\boldsymbol{\eta}(t^*) \tag{19}$$

where $\boldsymbol{U}$ is the right modal matrix and $\boldsymbol{\eta}_i(t) i = 1, 2, \ldots 2n_q$ are the modal coordinates. Inserting equation (19) into equation (17) and multiplying on the left by $\boldsymbol{V}^T$, we obtain the instantaneous modal equations:

$$\dot{\boldsymbol{\eta}}(t^*) = \boldsymbol{\Lambda}\boldsymbol{\eta}(t^*) + \mathbf{Q}(t^*) \tag{20}$$

where

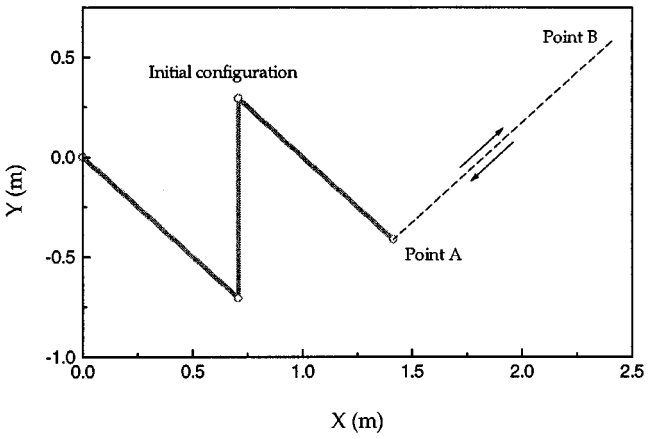
$$\boldsymbol{Q}(t^*) = \boldsymbol{V}^T\boldsymbol{B}^*\boldsymbol{f}_c^* = \boldsymbol{V}_L^T(\boldsymbol{M}_{qq}^*)^{-1}\boldsymbol{f}_c^* \tag{21}$$

is an instantaneous modal force, in which $\boldsymbol{V}_L$ is an $n_q \times 2n_q$ matrix representing the lower half of the left modal matrix $\boldsymbol{V}$. The eigenvalues and eigenvectors appear in pairs of complex conjugates. Hence, letting $\boldsymbol{v}_{L,j} \in R^{n_q}$ represent the lower half of the j-th left eigenvector, the associated complex conjugates are rewritten as

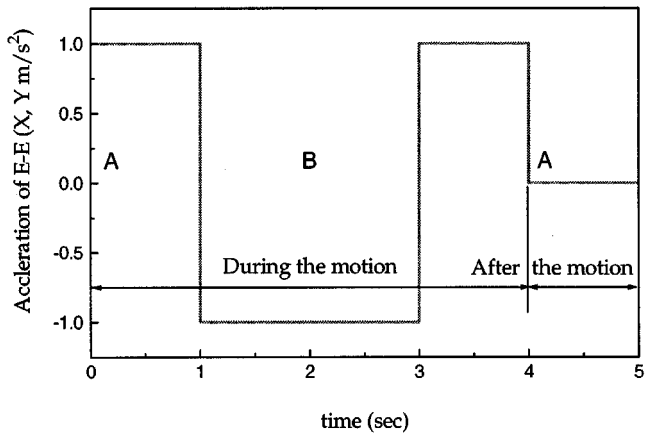
$$\boldsymbol{v}_{L,j+n} = \bar{\boldsymbol{v}}_{L,j}, \; j = 1, 2, \ldots n_q \tag{22}$$

The lower half of the left modal matrix can be arranged conveniently into the real and imaginary parts:

$$\boldsymbol{V}_{RI} = [\boldsymbol{V}_{RI,1}\boldsymbol{V}_{RI,2} \cdots \boldsymbol{V}_{RI,n_q}] \tag{23}$$



(a) The end effector trajectory and its initial configuration



(b) The end-effector acceleration profile

Fig. 5. The acceleration and position profile of the desired end-effector trajectory

$$\boldsymbol{V}_{RI,j} = [\mathrm{Re}\ \boldsymbol{v}_{L,j}\ \mathrm{Im}\ \boldsymbol{v}_{L,j}] \in R^{n_q \times 2}, \; j = 1, 2, \ldots, n_q \tag{24}$$

Replacing $\boldsymbol{f}_c^*$ with the r.h.s. of equation (13), the instantaneous modal force with respect to the selected lower modes (ρ) can be written as

$$\boldsymbol{Q}_\rho(t) = -\boldsymbol{V}_{RI,\rho}^T\boldsymbol{M}_{qq}^{*-1}\boldsymbol{M}_{qr}^*\boldsymbol{Z}\boldsymbol{\varepsilon}^* - \boldsymbol{V}_{RI,\rho}^T\boldsymbol{M}_{qq}^{*-1} \times \{\boldsymbol{M}_{qr}^*\boldsymbol{J}_r^+(\ddot{\boldsymbol{x}}_d^* + \boldsymbol{k}_v\dot{\boldsymbol{e}}^* + \boldsymbol{k}_p\boldsymbol{e}^* - \dot{\boldsymbol{J}}_r\dot{\boldsymbol{\theta}}^*) + N_q^*\} \tag{25}$$

In order to perfectly nullify the exciting modal forces, equation (25) should be zero, and then the self-motion vector can be obtained as

$$\boldsymbol{\varepsilon}^* = (\boldsymbol{H}^*)^+\boldsymbol{b}^* \tag{26}$$

where

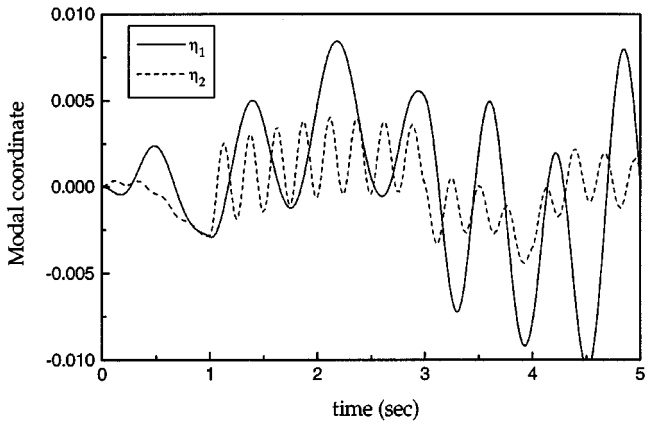
$$\boldsymbol{H}^* = \underbrace{\boldsymbol{V}_{RI,\rho}^T\boldsymbol{M}_{qq}^{*-1}\boldsymbol{M}_{qr}^*\boldsymbol{Z}}_{(R^{2\rho\times n_q}\cdot R^{n_q\times n_q}\cdot R^{n_q\times n_r}\cdot R^{n_r\times\rho})} \in R^{2\rho\times\rho},$$

$$(\boldsymbol{H}^*)^+ = (\boldsymbol{H}^{*T}\boldsymbol{H}^*)^{-1}\boldsymbol{H}^*$$

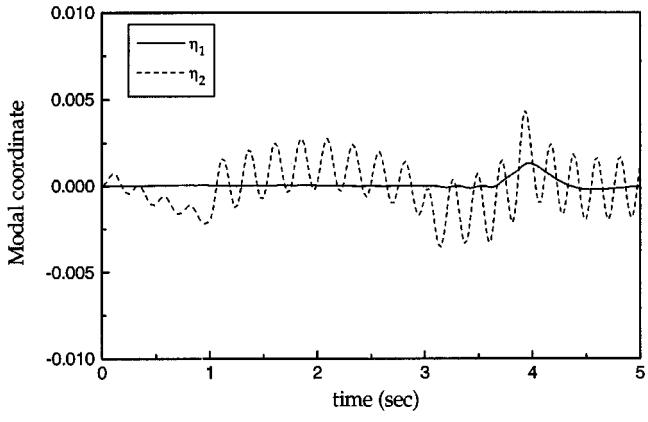
$$\boldsymbol{b}^* = -\boldsymbol{V}_{RI,\rho}^T\boldsymbol{M}_{qq}^{*-1}[\boldsymbol{M}_{qr}^*\boldsymbol{J}_r^+(\ddot{\boldsymbol{x}}_d^* + \boldsymbol{k}_v\dot{\boldsymbol{e}}^* + \boldsymbol{k}_p\boldsymbol{e}^* - \dot{\boldsymbol{J}}_r\dot{\boldsymbol{\theta}}^*) + N_q^*],$$

$$\boldsymbol{V}_{RI,\rho} = [\boldsymbol{V}_{RI,1} \cdots \boldsymbol{V}_{RI,\rho}]$$

The selected eigenvector matrix $\boldsymbol{V}_{RI,\rho}$ is composed of 2ρ column vectors of the selected lower modes. Another alternative is to evaluate the self-motion vector as a complex



(a) The self-motion obtained from equation (16) - Pseudo inverse solution



(b) The self-motion obtained from equation (26) - Modal force nullifying solution

Fig. 6. Comparison of the modal coordinates (solid line: η_1, dashed line: η_2)

https://doi.org/10.1017/S0263574798000770 Published online by Cambridge University Press

value

$$\boldsymbol{\varepsilon} = [\mathrm{Re}\ \varepsilon_1\ \mathrm{Im}\ \varepsilon_1 \cdots \mathrm{Re}\varepsilon_\rho\ \mathrm{Im}\ \varepsilon_\rho] \in R^{2\rho} \quad (27)$$

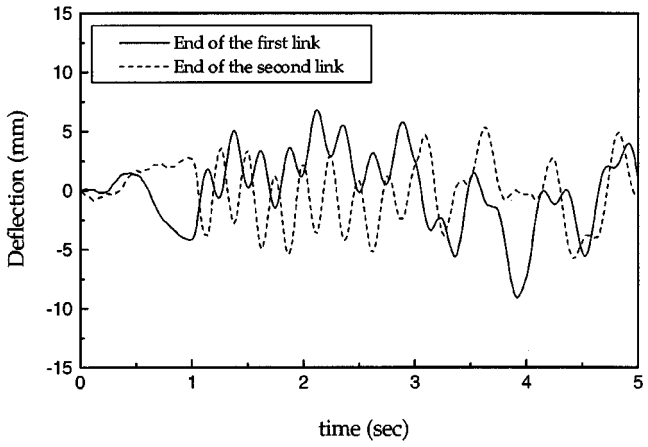
$$\boldsymbol{\varepsilon}^* = (\boldsymbol{H}^*)^{-1}\boldsymbol{b}^* \quad (28)$$

Then, only the real part is taken as the self-motion vector because the imaginary part cannot be realized.

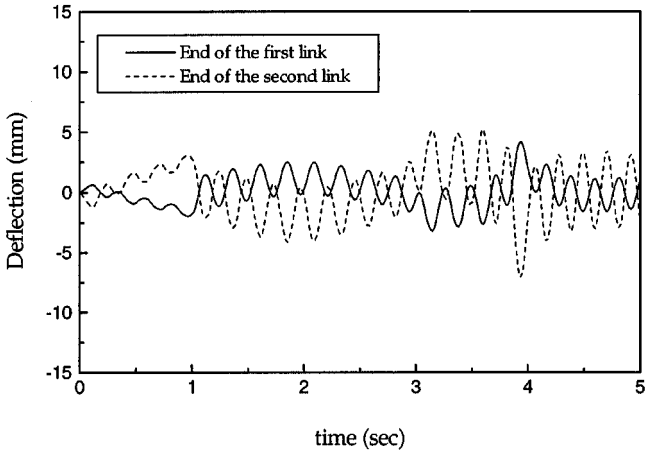
4. NUMERICAL SIMULATION

The planar structurally flexible redundant manipulator shown in Figure 1 is used to demonstrate the effectiveness of self-motion utilization for reducing motion-induced vibration during and after a given motion. The first and second links are flexible possessing an in-plane transverse motion, and the third link is assumed rigid, having one DOF. The parameters of the manipulator are listed in Table I. Thus, this sytem has one DOR: $n_r=3$, $m=2$, $\rho=1$.

Two sets of simulations are presented. In the first set, when the end-effector is desired to maintain a stationary point, the self-motion utilization is compared with the full state regulation control algorithm for the linearized system. In the second set, the effectiveness of the modal approach is compared with the pseudo-inverse approach[3] with respect to a continuous path tracking task.



(a) The self-motion obtained from equation (16) - Pseudo inverse solution

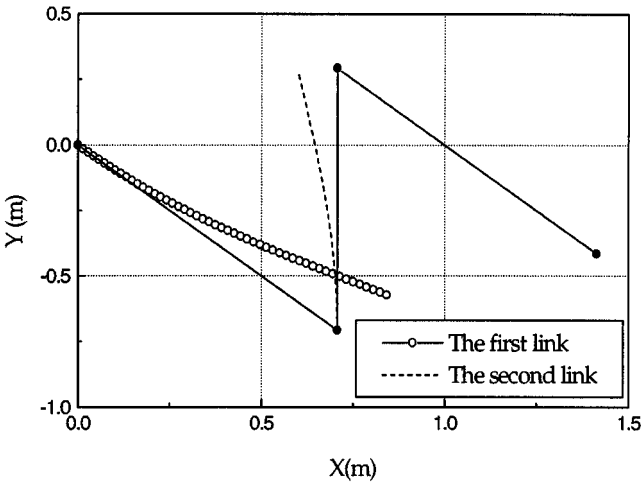


(b) The self-motion obtained from equation (26) - Modal force nullifying solution

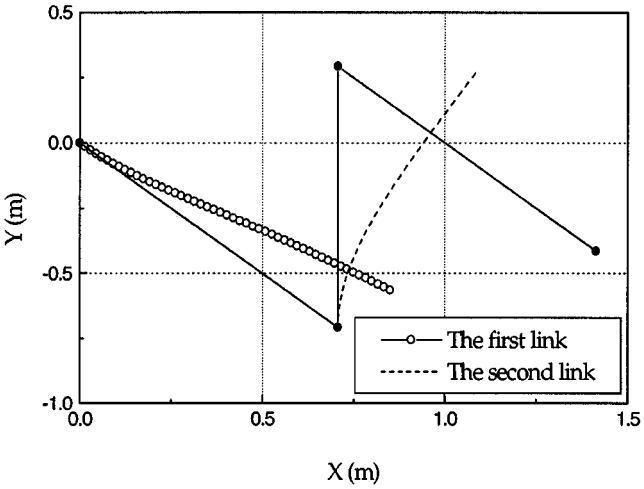
Fig. 7. Deflection at the first and the second flexible link (solid line: the first link, dashed line: the second link)

4.1. *Positioning at the stationary point*

Let's assume that the end-effector is positioned at a stationary point $\mathbf{B}(X,Y)=(1+\sqrt{2},2-\sqrt{2})$ in an inertia reference frame. The manipulator is assumed to be in one of many possible configurations: $\theta_{ref}^T=\{-0.205, 1.319,$



(a) The first mode (2.07 Hz)



(b) The second mode (4.29 Hz)

Fig. 8. Mode shapes of the flexure motion (solid line: rigid link configuration, circle: the first link, dashed line: the second link)

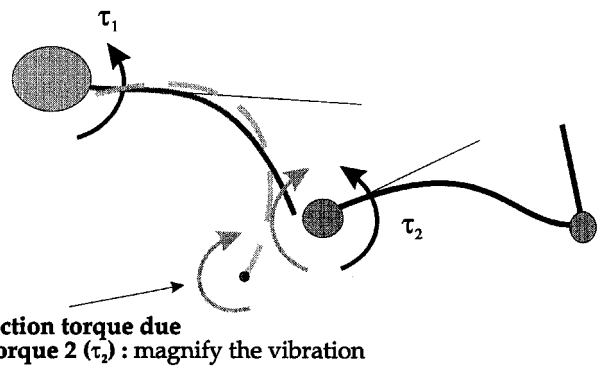


Fig. 9. When the joint torques at joints 1 and 2 are going in the same direction (solid gray line: deflection due to τ_1, dashed gray line: deflection due to the reaction torque of τ_2).

https://doi.org/10.1017/S0263574798000770 Published online by Cambridge University Press

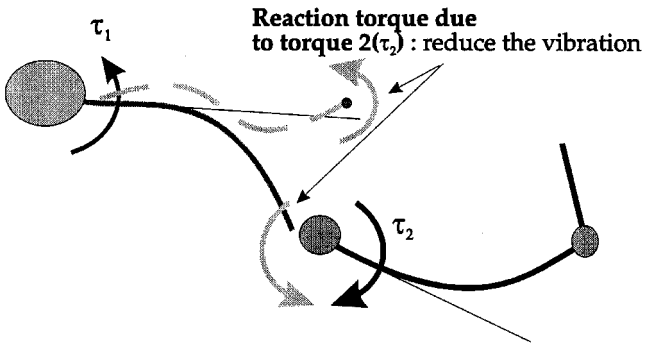


Fig. 10. When the joint torques at joints 1 and 2 are going in the opposite direction (solid gray line: deflection due to τ_1, dashed gray line: deflection due to the reaction torque of τ_2).

$-1.222\}$. When the second link is suddenly excited ($\dot{q}_{21}=0.01$ initially), the manipulator is required to damp out the flexure motion while maintaining the end-effector point at the stationary point **B**.

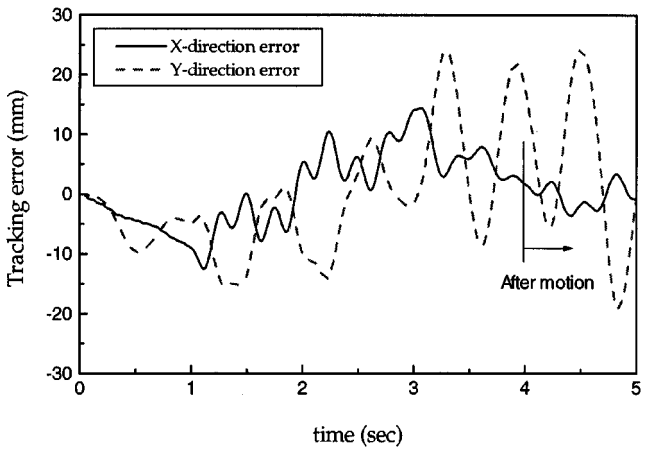
The proposed control strategy of self-motion utilization (using equations (26)), is compared with the full state feedback method. The feedback controller is designed for the linearized system using the well-known LQR design method so as to minmize the performance index, J;

$$J=\int_0^\infty \left[\begin{Bmatrix} \delta\boldsymbol{\theta} \\ \boldsymbol{q} \end{Bmatrix}^T \mathbf{Q} \begin{Bmatrix} \delta\boldsymbol{\theta} \\ \boldsymbol{q} \end{Bmatrix} + \boldsymbol{\tau}_{com}^T \mathbf{R} \boldsymbol{\tau}_{com} \right] dt \qquad (29)$$

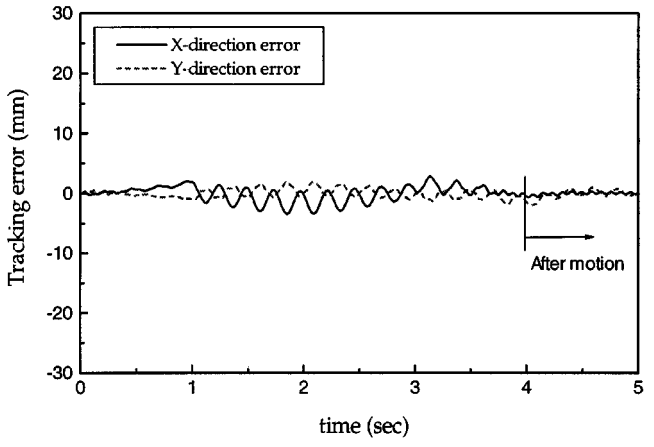
Then the joint torque can be expressed as

$$\boldsymbol{\tau}_{com} = -\mathbf{K}_{feed}\{\delta\boldsymbol{\theta}^T, \boldsymbol{q}^T, \delta\dot{\boldsymbol{\theta}}^T, \dot{\boldsymbol{q}}^T\}^T \qquad (30)$$

where $\delta\boldsymbol{\theta}=\boldsymbol{\theta}-\boldsymbol{\theta}_{ref}$ and the feedback gain matrix $\mathbf{K}\in R^{n_r\times 2n}$ can be calculated by the pole placement technique or other methods. The comparison is shown in Figures 2–4. As shown in Figure 3, the full state feedback can reduce the deflection of the flexible link faster than self-motion utilization. However, the end-effector position error is considerably larger (Figure 4) than that obtained from the proposed method. This is because the joint torque not only reduces the vibration, but it also affects the end-effector motion. Even though a minimal amount of vibration remains at the flexible links, it cannot guarantee the reduction of end-effector position error. On the other hand, in the self-motion utilization method, the joint torques actuate in the null space of the Jacobian matrix; the vibration is reduced while not affecting the end-effector motion. As a result, the tracking error of the end-effector can be drastically reduced even though the deflection of the flexible links are not reduced completely.



(a) The self-motion obtained from equation (16) - Pseudo inverse solution



(b) The self-motion obtained from equation (26) - Modal force nullifying solution

Fig. 11. Comparison of tracking error of the end-effector during and after motion (solid line: X direction error, dashed line: Y direction error)

4.2. Continuous path tracking

The trajectory of the end-effector which is frequently used to test joint torque optimization problems[13,14] is shown in Figure 5. With constant bang-bang type acceleration (1 m/s^2) the end-effector moves back and forth in a straight line from point A ($\sqrt{2}$, $1-\sqrt{2}$) to point B ($1+\sqrt{2}$, $2-\sqrt{2}$) in 2 sec and then returns to point A in the same time period.

In order to test the effectiveness of the modal space approach, two methods are compared: the pseudo-inverse solution equation (16) and the modal force nullifying soution equation (26).

The 1st and 2nd modal coordinates defined in modal space by equation (19) are compared in Figure 6. The pseudo-inverse solution cannot nullify the inertia force completely because it is obtained in a least squares sense. Therefore, it cannot alter the flexure motion as shown in equation (14). On the other hand, the modal approach can nullify the dominant modal force completely with respect to selected ρ low modes. In this case the available DOR is one, so the 1st modal force can be nullified according to equation (26). With respect to selected ρ nodes, the flexure motion equation can be altered as shown in equation (26). As a result, the 1st modal coordinate is significantly reduced (Figure 6-b).

The advantage of the modal space approach is more noticeable when the deflections at the end of the 1st and 2nd flexible links are compared, as shown in Figure 7. In the pseudo-inverse solution the deflection is complex and does not show any periodic tendencies. However, the modal space approach shows smaller deflections and a regular pattern. The deflections are almost phased out because the

https://doi.org/10.1017/S0263574798000770 Published online by Cambridge University Press

1st mode of flexure motion is nullilfied (as illustrated in Figure 6-b). The 1st mode component (2.07 Hz) of the flexure motion is eliminated and the 2nd mode component (4.29 Hz) becomes dominant.

This characteristic can be explained using the mode shapes of the flexure motion. Figure 8 represents the vibration mode of the flexure motion defined in equation (19). The 1st mode shape (Figure 8-a) is the in-phase motion between the 1st and 2nd links, while the 2nd mode shape (Figure 8-b) is the out-of-phase motion.

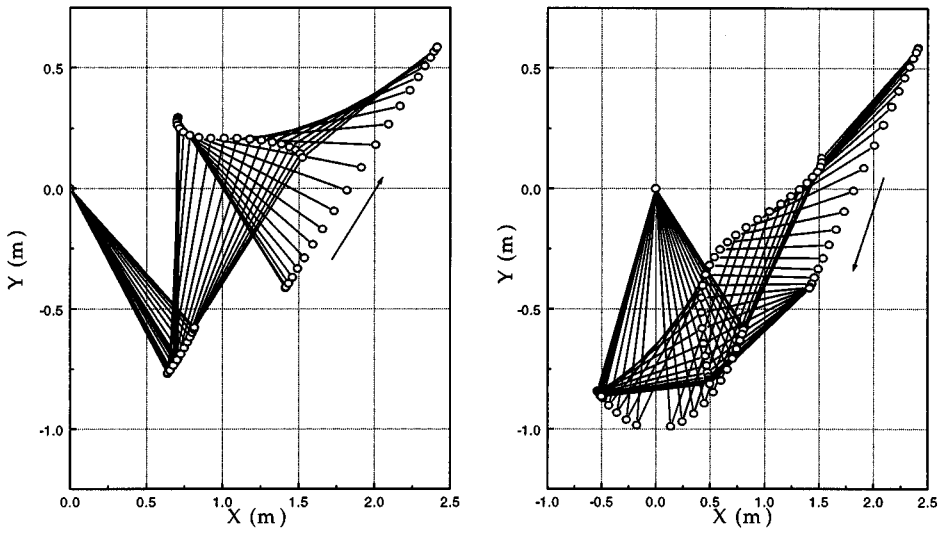
The in-phase motion (both τ_1 and τ_2) is physically interpreted as Figure 9. Due to the inertia force, the 1st link will deflect in an opposite direction to the joint torque (τ_1). The reaction torque induced by the next outward joint torque (τ_2) will make the inward link deflect as shown by the dashed line. By comparison, Figure 10 shows that in the out-of-phase motion (τ_1 is counterclockwise and τ_2 is clockwise), the reaction torque reduces the deflection at the end of the inward link.

Because self-motion is utilized to nullify the 1st modal force, the in-phase mode (1st mode) is eliminated but the out-of-phase mode (2nd mode) remains. Thus the deflection at the end of the links are phased out (Figure 9-b). This result is beneficial to the reduction of tracking errors during motion as shown in Figure 11-a,b.

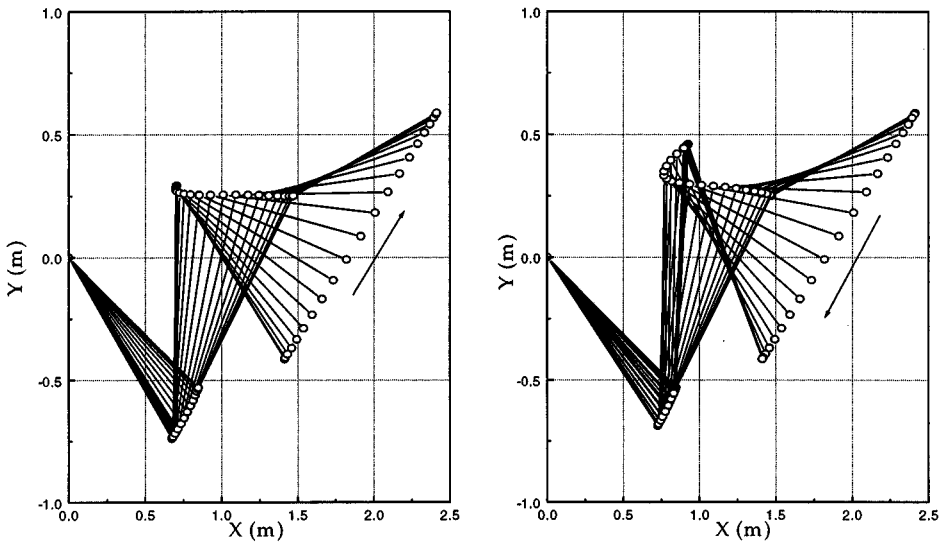
It can be observed that both the tracking errors and the residual vibration after the motion are considerably reduced. It is not surprising that the magnitude of deflection (Figure 7-a/b) is approximately of the same order but the magnitude of the tracking error (Figure 11-a/b) is considerably different.

When the manipulator arms are composed in serial, the in-phase deflection at the end of the inward links magnify the tracking error of the end-effector. On the other hand, the out-of-phase deflection can reduce the tracking error even though the deflection is not eliminated completely.

The back and forth motion of the manipulator and its residual vibration are shown in Figure 12. Compared to the pseudo-inverse solution approach, the modal space approach shows that the manipulator configuration is well



(a) The self-motion obtained from equation (16) – Pseudo inverse solution



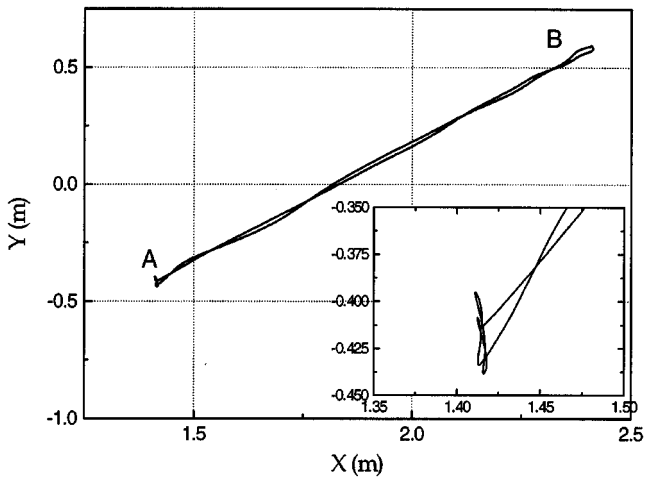
(b) The self-motion obtained from equation (26) – Modal force nullifying solution

Fig. 12. The outgoing and returning motion profile.

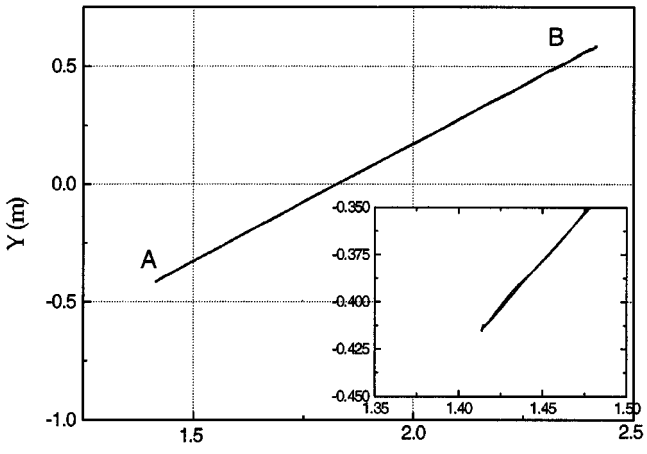
https://doi.org/10.1017/S0263574798000770 Published online by Cambridge University Press

preserved and its residual vibration is considerably reduced after the motion. The locus of motion is compared in Figure 13. The desired motion of the end-effector is a straight line between points A and B. The residual vibration is magnified in the inner box.

The simulation above concludes that self-motion can be utilized to suppress the vibration of flexible links by nulifying the dominant modal force induced by rigid body motion. Self-motion can alter the joint motion while simultaneously not affecting the end-effector motion. Therefore, the proposed approach is beneficial to reducing the tracking error. The magnitude of low mode components of flexural motion is considerably larger than those of the remaining high mode components. Recognizing this fact, the modal space approach, which nullifies the low modal force in modal space, is more effective and superior to the pseudo-inverse approach.



(a) The Pseudo inverse solution



(b) The modal force nullifying solution

Fig. 13. The locus of end-effector.

5. CONCLUDING REMARKS

A new tracking control algorithm for structurally flexible redundant manipulators utilizing their self-motion capabilities was proposed. In modal space, the dynamic effects of self-motion on the flexure motion of manipulators was investigated. In the proposed algorithm, self-motion is utilized in order to nullify the dominant modal force of flexural motion that is induced by rigid body motion. Therefore, self-motion can alter the dynamics of flexure motion while simultaneously not affecting the end-effector motion. The results presented show that the modal space approach is effective in reducing the tracking error and is more beneficial and superior to the pseudo-inverse approach, when the DOF is restricted to one or two.

References

1. D.N. Nenchev, "Redundancy Resolution through Local Optimization: A Review" *J. of Robotic Systems* **6**, 769–798 (1989).
2. W.J. Book, "Controlled Motion in an Elastic World" *Trans. ASME J. of Dynamic Systems, Measurement, and Control*, **113**, 252–261 (1993).
3. L.A. Nguyen, I.D. Walker and R.J.P. DeFigueriredo, "Dynamic Control of Flexible Kinematically Redundant Robot Manipulators" *IEEE Trans. on Robotics and Automation*, **8**(6), 759–767 (1992).
4. E. Barbieri and Q. Wang, "An Example of Optimal Set-point Relegation for Self-motion Control in Redundant Flexible Robots" *Proc. IEEE. Inter. Conf. on Robotics and Automation* (1990), pp. 632–637.
5. J. Carusone and G.M.T. D'Eleuterio, "Tracking Control for End-Effector Position and Orientation of Structurally Flexible Manipulators" *J. of Robotics System* **10**(6), 847–870 (1993).
6. T. Yoshikawa, K. Hosoda, T. Doi and H. Murakami, "Quasi-Static Trajectory Tracking Control of Flexible Manipulator by Macro-Micro Manipulator System" *Proc. IEEE, Inter. Conf. on Robotics and Automation* (1993) **3**, pp. 210–215.
7. S.J. Kim and Y.S. Park, "Motion resolution of flexible, redundant robot manipulators for vibration reduction" *Proc. 3rd Inter. Conf. on Motion and Vibration Control* (1996) **1**, pp. 251–256.
8. R.D. Blevins, *Formulas for National Frequency and Mode Shape* (Van Nostrand Reinhold Company, 1979).
9. A.R. Fraser and R.W. Daniel, *Perturbation Techniques for Flexible Manipulators* (Kluwer Academic Publishers, Dordrecht, 1991).
10. P.H. Chang, "Closed-form Solution for Inverse Kinematics of Robot Manipulator with Redundancy" *IEEE Trans. on Robotics and Automation* **RA-3**(5), 393–403 (1987).
11. L. Meirovitch, *Dynamics and Control of Structures* (John Wiley & Sons, New York, 1990).
12. A.M. Browder and R.M. Alexander, "A General Approach to Modal Analysis for Time Varying Ssytems," *AIAA paper 88–2356* (1988) pp. 1162–1168.
13. H.J. Kang and R.A. Freeman, "Null Space Damping Method for Local Joint Torque Optimization of a Redundant Manipulators" *J. of Robotic System* **10**(2), 249–270 (1993).
14. J.M. Hollerbach and K.C. Suh, "Redundancy resolution of manipulators through torque optimization" *Proc. IEEE Inter. Conf. on Robotics and Automation* (1985) **2**, pp. 1016–1021.

https://doi.org/10.1017/S0263574798000770 Published online by Cambridge University Press